Supporting Information

Ethanol-assisted room-temperature rapid self-healing polydimethylsiloxane-polyurea/carbon composite elastomers for energy harvesters and smart sensors

*Yiming Du,[ab] Hua Wang,[*a] Xiaofei Li,[ab] Jincheng Liu,[ac] Yanyan Liu,[a] Wei Zhang,[a] Qiang Liu,[ab] Yunsheng Da,[ab] Hao Li,[ab] Zhouping Sun,[ab] Yong Dong[ab] and Xingyou Tian [a]*

[a] *Institute of Solid State Physics, Hefei Institutes of Physical Science, Chinese Academy of Sciences, Hefei 230031, China*

[b] *University of Science and Technology of China, Hefei 230026, China*

[c] *Institutes of Physical Science and Information Technology, Anhui University, Hefei, Anhui 230601, China*

**Corresponding author e-mail: wanghua@issp.ac.cn*

Supporting information is included as follows:

Supporting Figs. S1- S15 and Tables. S1-S4.

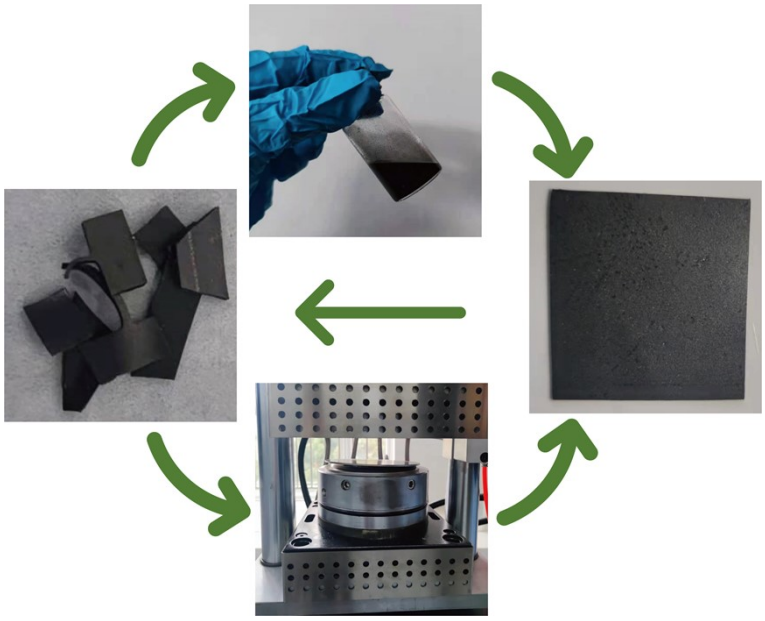

Fig. S1. Recycle of CCF/PDMS by dissolution and hot pressing.

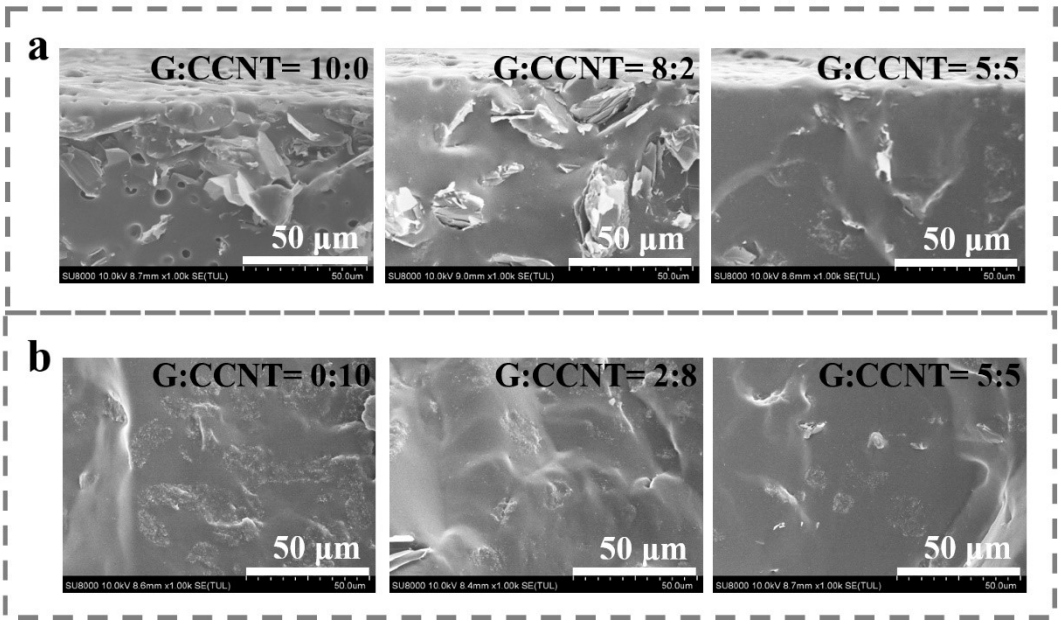

Fig. S2. The cross-sectional SEM images of composite films with different G to CCNT ratios: (a) Dispersion of graphite at the bottom of the films, (b) Dispersion of CCNT in films.

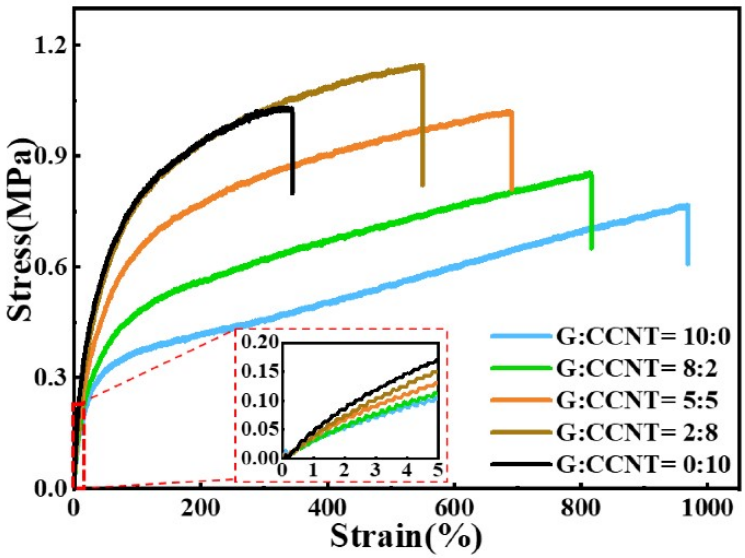

Fig. S3. Typical strain-stress curves of composite films with different G to CCNT ratios.

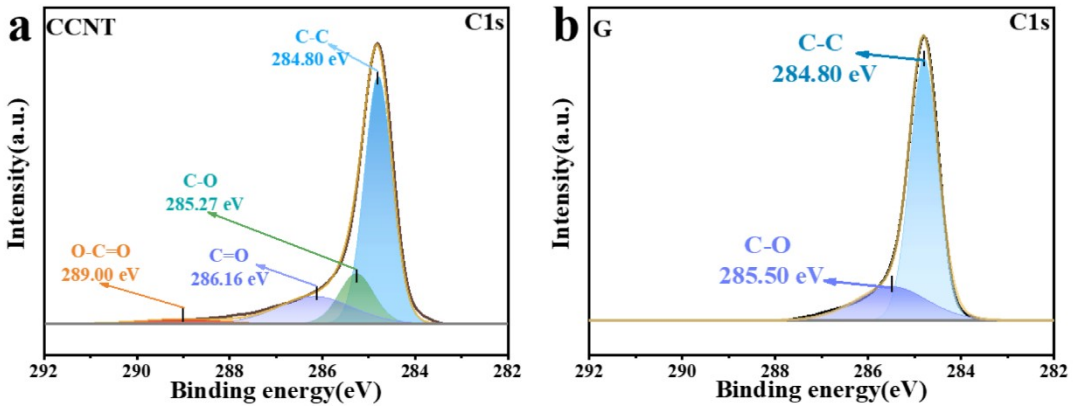

Fig. S4. XPS fitting curves of C 1s of (a) CCNT, (b) G

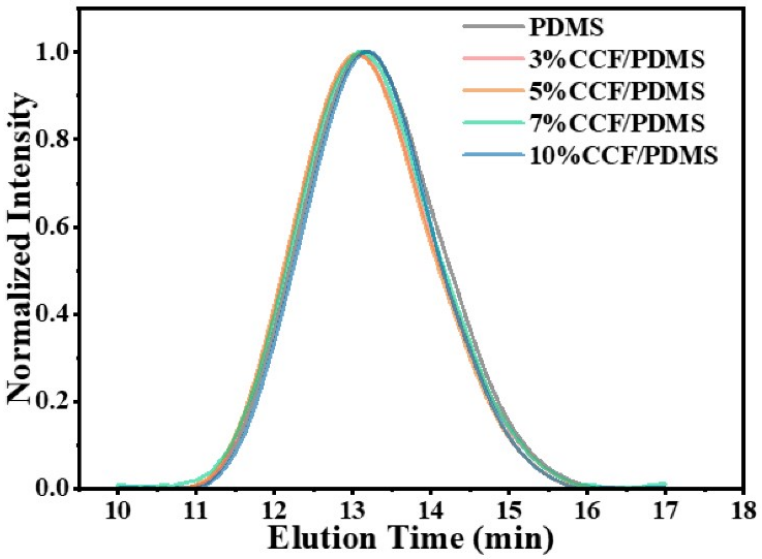

Fig. S5. GPC curves of PDMS and CCF/PDMS films

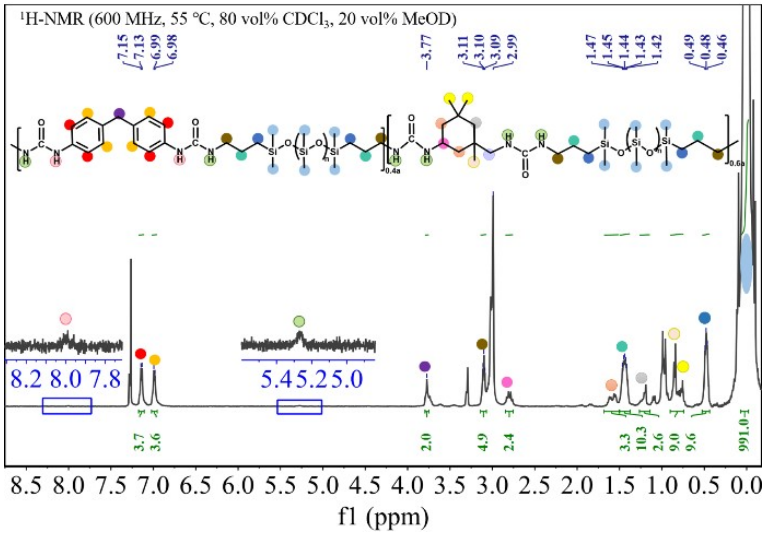

Fig. S6. 1H-NMR spectra of synthesized PDMS (600MHz, 55 ℃，80 vol%CDCl3, 20 vol%MeOD): δ 7.15(CH of MDI), 7.13(CH of MDI), 6.99, 6.99, 3.77, 3.11, 3.10, 3.09, 2.99, 1.47, 1.45, 1.44, 1.43, 1.42, 0.49, 0.48, 0.46.

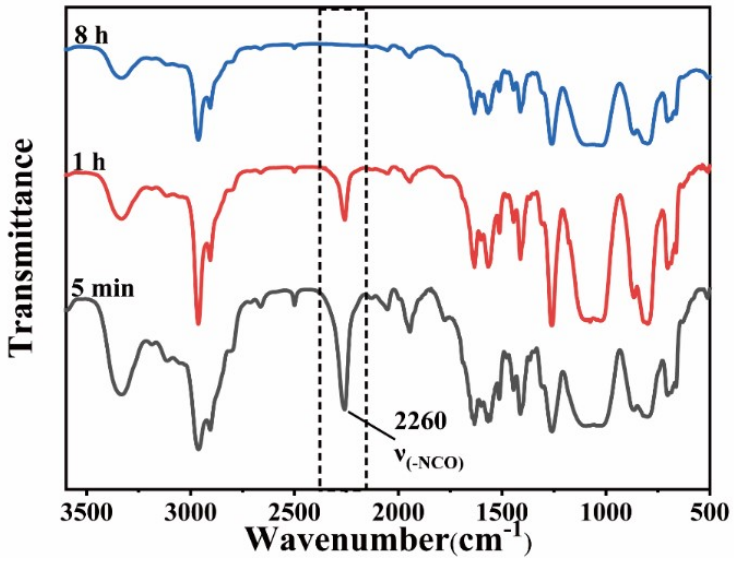

Fig. S7. FTIR spectra of PDMS during preparation.

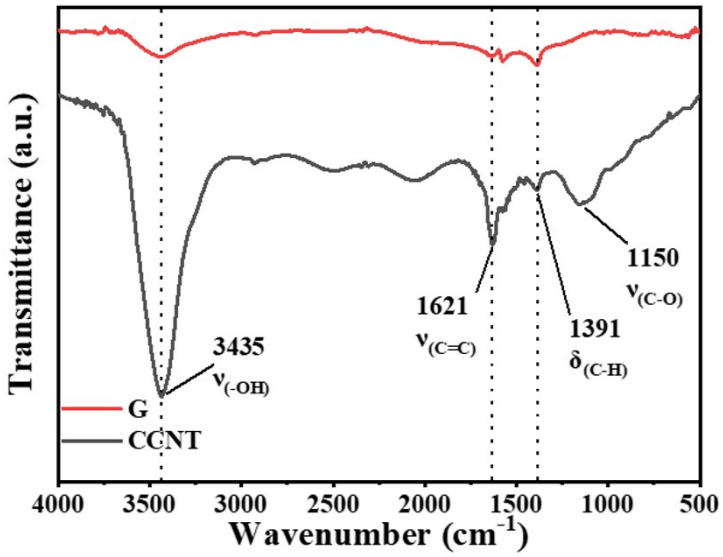

Fig. S8. FTIR spectra of G and CCNT.

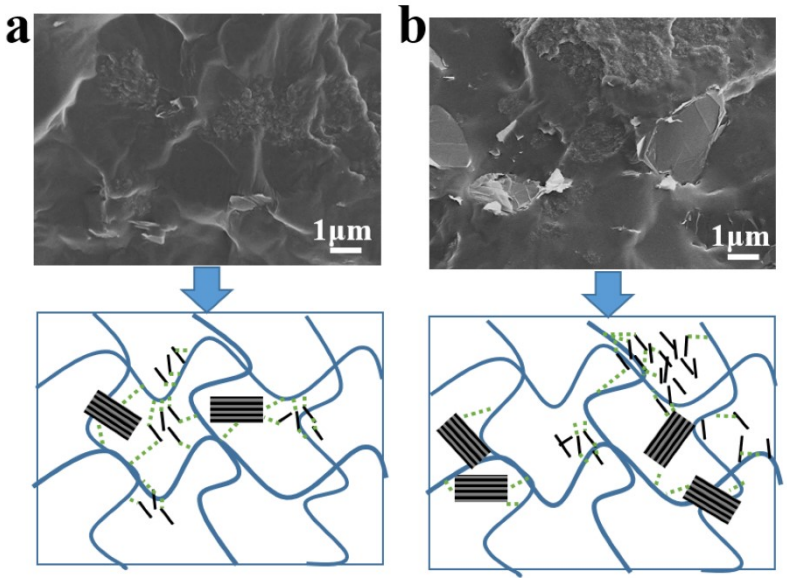

Fig. S9. SEM and illustration of (a) 5%CCF/PDMS, (b) 10%CCF/PDMS

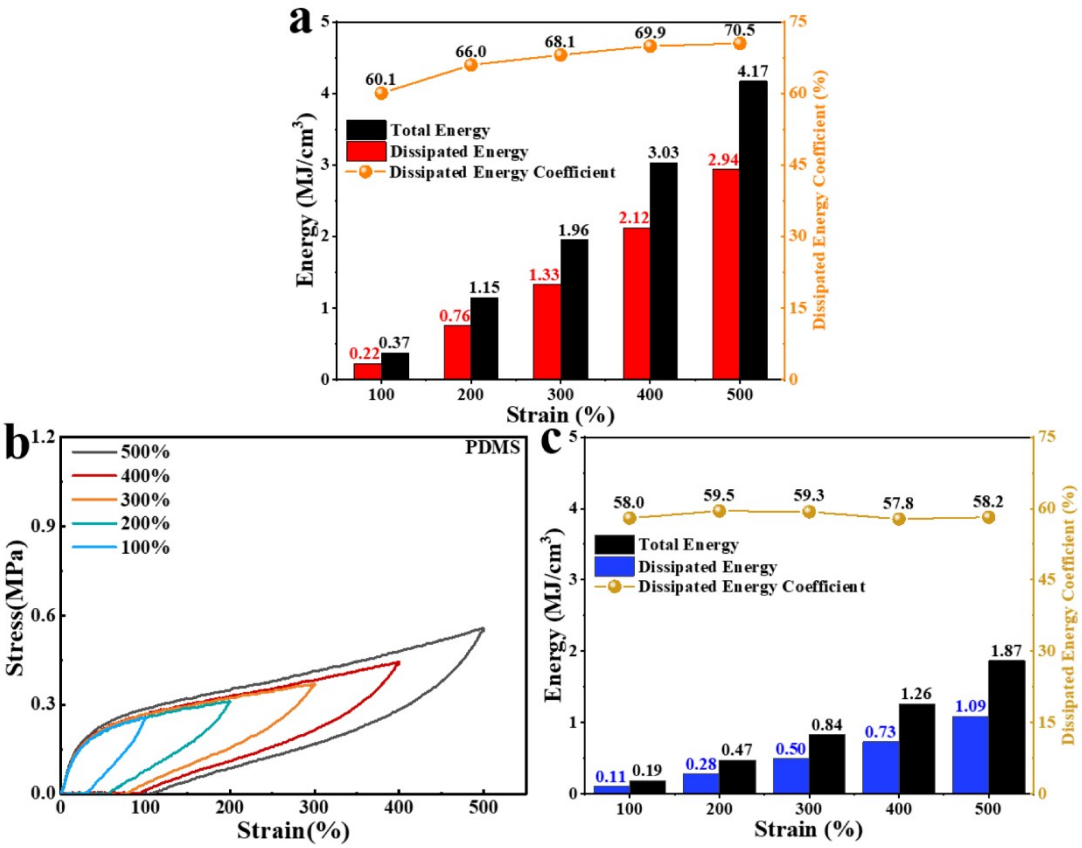

Fig. S10. (a) Toughness and energy dissipation ratio of 5%CCF/PDMS under different strains (100%, 200%, 300%, 400% and 500%). (c) Loading-unloading curves and (c) corresponding toughness and energy dissipation ratio of PDMS under different strains (100%, 200%, 300%, 400% and 500%).

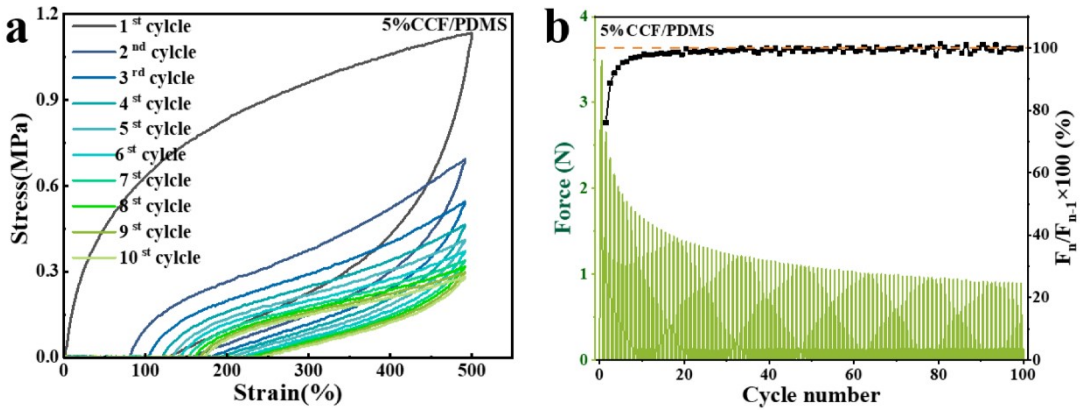

Fig. S11. Loading-unloading curves of 5%CCF/PDMS subjected to 10 cycles of stretching at a strain of 500%. (b)Load of 5%CCF/PDMS during 100 cycles of stretching at a fixed strain (200%).

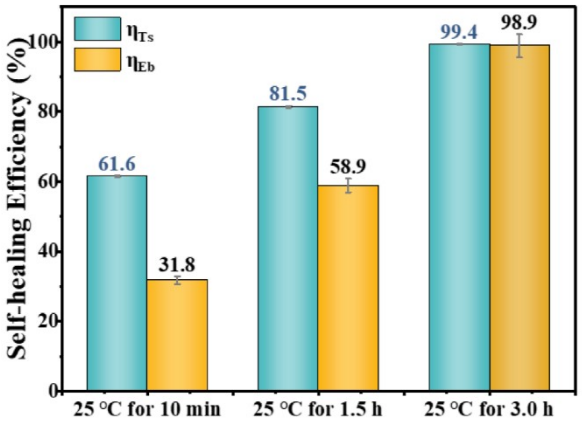

Fig. S12. Self-healing efficiency of ethanol-assisted self-healing

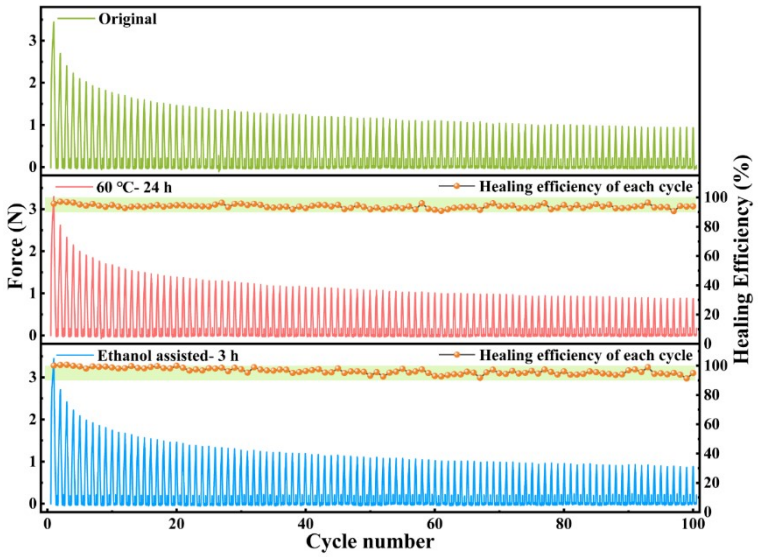

Fig. S13. Cyclic stretch curves of 5%CCF/PDMS before and after healing (200%, 100 cycles).

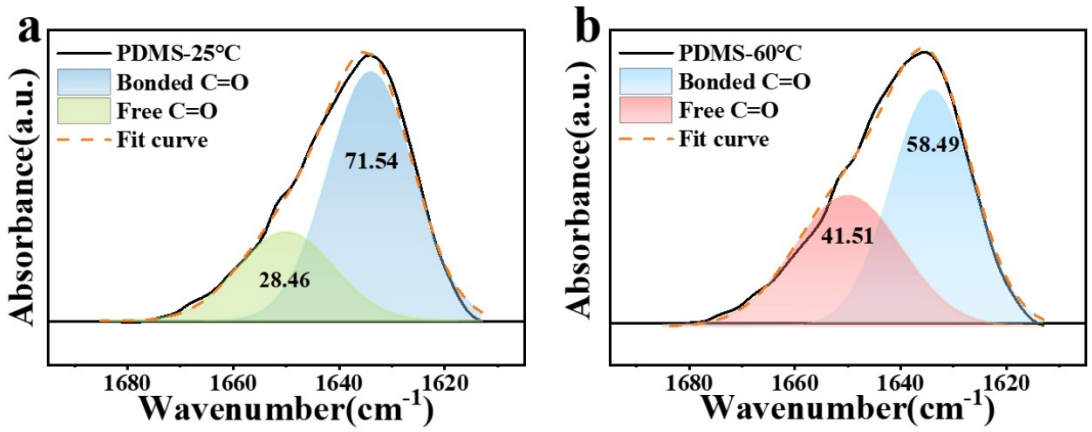

Fig. S14. In situ FTIR spectra of PDMS at (a) 25℃, (b) 60℃.

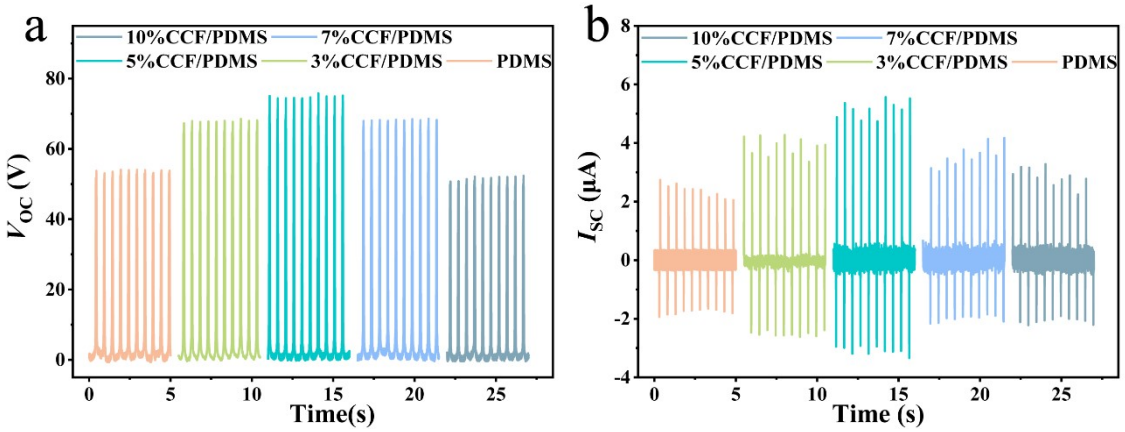

Fig. S15. (a) Voltage output and (b) short-circuit current of SH-TENG based on X%CCF/PDMS films with various CCF contents.

Table. S1. Mechanical properties of composite films with different G to CCNT ratios.

G: CCNT	Toughness (MJ ·m-3)	Young's modulus (MPa)	Tensile strength (MPa)	Elongation at break (%)
10: 0	5.20±0.20	2.03±0.042	0.78±0.018	912±63.6
8: 2	5.54±0.33	2.18±0.064	0.86±0.014	837±36.8
5: 5	**5.63±0.53**	**2.62±0.011**	**1.02±0.018**	**680±52.4**
2: 8	5.37±0.20	3.03±0.075	1.15±0.005	575±37.5
0: 10	2.84±0.20	3.45±0.056	1.04±0.014	331±12.3

Table. S2. Summary of the molecular weight according to GPC results.

CCF	M_n	M_w	PDI
PDMS	58038	118297	2.0
3%CCF/PDMS	59222	131347	2.2
5%CCF/PDMS	60310	109802	1.8
7%CCF/PDMS	59898	133084	2.2
10%CCF/PDMS	58639	113758	1.9

Table. S3. Mechanical properties of composite films with different filler contents.

CCF	Young's modulus (MPa)	Tensile strength (MPa)	Elongation at break (%)	Toughness ($MJ \cdot m^{-3}$)
PDMS	0.74±0.02	0.66±0.04	1103.6±64.6	5.10±0.25
3%CCF/PDMS	1.10±0.03	0.82±0.04	882.5±13.4	4.89±0.24
5%CCF/PDMS	1.53±0.05	1.02±0.01	687.9±22.6	5.43±0.27
7%CCF/PDMS	2.17±0.02	1.05±0.01	583.0±42.53	5.00±0.41
10%CCF/PDMS	2.61±0.02	0.97±0.01	311.1±23.48	2.42±0.18

Table. S4. Mechanical properties of various solvent assisted self-healing polymers.

Materials (solvent)	Elongation at break (%)	Tensile strength (MPa)	Healing time (h)	Healing efficiency (%)		Ref.
				η_{EB}	η_{TS}	
5%CCF/PDMS (Ethanol)	687.9	1.02	3	98.9	99.4	This work
			1.5	58.9	81.5	
			0.17	31.8	61.6	
30 wt% P3HT (THF vapor)	~38	~2.0	0.5	~75	~75	1
UPy-CPU-2 (IPA)	2340	9.44	12	79.7	59.0	2
PDMS-Boroxine (Water, 60°C)	9.93	10.04	12	73.0	85.2	3
CAO-1.6 (Dioxane, 90°C)	~600	0.3	12	92	~100%	4
PVA-C6-gel (Hot ethanol/H_2O, v/v = 1:1)	333	3.9	12.17	~100	~100	5
N40 (Methanol)	138	1.8	48	8.0	28.9	6
HHIF-Zn (RH = 95%)	213	13.49	24	97.7	88.1	7

~: Estimated values from figures.

References

1 P. Baek, N. Aydemir, O. J. Chaudhary, E. Wai Chi Chan, J. Malmstrom, T. Giffney, R. Khadka, D. Barker and J. Travas-Sejdic, *RSC Advances*, 2016, **6**, 98466-98474.

2 M. W. M. Tan, G. Thangavel and P. S. Lee, *Advanced Functional Materials*, 2021, **31**, 2103097.

3 J.-C. Lai, J.-F. Mei, X.-Y. Jia, C.-H. Li, X.-Z. You and Z. Bao, *Advanced Materials*, 2016, **28**, 8277-8282.

4 S. Debnath, C. Upadhyay and U. Ojha, *ACS Applied Materials & Interfaces*, 2022, **14**, 9618-9631.

5 S. Wang, M. Liu, L. Gao, G. Guo and Y. Huo, *ACS Applied Materials & Interfaces*, 2019, **11**, 19554-19564.

6 S. Nakagawa, S. Nakai, K. Matsuoka and N. Yoshie, *Polymer*, 2019, **161**, 101-108.

7 J. Xu, S. Ye and J. Fu, *Journal of Materials Chemistry A*, 2018, **6**, 24291-24297.